Molecular Pharmacology Fast Forward. Published on March 13, 2008 as doi:10.1124/mol.107.041590


MOL #41590

# A Role for Leu118 of Loop E in Agonist Binding to the α7 Nicotinic Acetylcholine Receptor

Shiva Amiri*, Masaru Shimomura*, Ranjit Vijayan, Hisashi Nishiwaki, Miki Akamatsu, Kazuhiko Matsuda, Andrew K. Jones, Mark S.P. Sansom, Philip C. Biggin and David B. Sattelle.

[1]Structural Bioinformatics and Computational Biochemistry Unit, Department of Biochemistry, University of Oxford, South Parks Road, Oxford OX1 3QU (SA, MSP and PCB)

[2]Department of Applied Biological Chemistry, School of Agriculture, Kinki University (MS and KM)
Graduate School of Agriculture, Kyoto University, Kita-shirakawa, Sakyo-Ku, Kyoto 606-8502, Japan (MA)

[3]Department of Physiology, Anatomy and Genetics, Le Gros Clark Building, University of Oxford, South Parks Road, Oxford OX1 3QX, UK (AKJ and DBS)

*These authors have contributed equally to this work.

Molecular Pharmacology Fast Forward. Published on March 13, 2008 as DOI: 10.1124/mol.107.041590
This article has not been copyedited and formatted. The final version may differ from this version.

MOL #41590

**Running title:** Role for Leu118 of loop E in nAChR-agonist interactions

To whom correspondence should be addressed:
David B. Sattelle
Tel: +44 (0) 1865 - 272 145
Fax: +44 (0)1865 - 272 421
Email: david.sattelle@anat.ox.ac.uk

For submission to Molecular Pharmacology, 21.06.2006



No. of text pages: 31

No. of tables: 2

No. of figures: 9

No. of words: 7,487

Abbreviations: ACh, acetylcholine; nAChR, nicotinic acetylcholine receptor; $EC_{50}$, half maximum concentration; $I_{max}$, maximum normalized response; $I_{min}$, minimum normalized response, $n_H$, Hill coefficient Abbreviations: AChBP, acetylcholine binding protein; DN-IMI, desnitro-imidacloprid; IMI, imidacloprid.

Molecular Pharmacology Fast Forward. Published on March 13, 2008 as DOI: 10.1124/mol.107.041590
This article has not been copyedited and formatted. The final version may differ from this version.



**Abstract.**

Nicotinic acetylcholine receptors (nAChRs) are ligand-gated ion channels mediating fast cholinergic synaptic transmission in the brain and at neuromuscular junctions. We used the structure of the acetylcholine binding protein (AChBP) from *Lymnaea stagnalis,* to model the chicken α7 agonist-binding domain. The initial models and a preliminary docking study suggested that position L118 may play an important role in determining agonist actions on α7. A prediction from these *in silico* studies, that L118E and L118D would retain binding to acetylcholine, but L118K and L118R would not, was confirmed in electrophysiological studies on functional recombinant mutant receptors expressed in *Xenopus laevis* oocytes. The functional studies also demonstrated that residues at position 118 have a dramatic effect on the actions of imidacloprid (a partial agonist of wild-type α7 receptors) and its des-nitro derivative. Molecular Dynamics simulations confirm that L118 can strongly influence agonistbinding and that the model is robust in terms of its prediction for acetylcholine binding. Together, the results indicate a role forL118 in in influencing agonist actions on α7nAChRs.

Molecular Pharmacology Fast Forward. Published on March 13, 2008 as DOI: 10.1124/mol.107.041590
This article has not been copyedited and formatted. The final version may differ from this version.



## Introduction

Nicotinic acetylcholine receptors (nAChRs) are plasma membrane cation channels activated by the neurotransmitter acetylcholine (ACh). They mediate fast cholinergic synaptic transmission at neuromuscular junctions and in the brain (Karlin, 2002; Lena and Changeux, 1998). The nAChR molecules are pentamers composed of identical or highly homologous subunits, each with four transmembrane regions (TM1-4) and an extracellular N-terminal domain containing 6 loops (A-F) that make up the ACh binding site (Corringer et al., 2000a). Subunits possessing two adjacent cysteines in loop C of the ACh binding site are designated α subunits, whereas those lacking this cysteine pair are denoted non-α or β subunits.

Neuronal nicotinic receptor subunits (α2-10; β2-4), which contribute to a variety of receptor subtypes depending on subunit composition (Millar, 2003a; Millar, 2003b), are important targets for new drugs (Arneric et al., 2007 Biochem Pharmacol 74,1092-1101). These include drugs being developed as analgesics and drugs for ameliorating the symptoms of Alzheimer's disease (Papke et al., 2000; Prendergast et al., 1998), as well as drugs used to treat Parkinson's disease and schizophrenia (Lloyd and Williams, 2000). Congenital myasthenias (Ohno and Engel, 2002) result from mutations in muscle nAChR subunits and autosomal nocturnal frontal lobe epilepsy results from mutations in neuronal α4 and β2 nAChR subunits (Changeux and Edelstein, 2001; Steinlein, 2001). Also, autoantibodies directed against nAChRs underlie several diseases such as myasthenia gravis (muscle nAChRs) (Lang and Vincent, 2003a; Lang and Vincent, 2003b), Rasmussen's encephalitis (α7) (Watson et al., 2005) and Autonomic Neuropathy (α3) (Vernino and Lennon, 2003a; Vernino and Lennon, 2003b). The nAChRs of insects are the targets for imidacloprid, a neonicotinoid insecticide extensively used worldwide (Matsuda et al., 2001b). In addition, nematode nAChRs are important targets for

Molecular Pharmacology Fast Forward. Published on March 13, 2008 as DOI: 10.1124/mol.107.041590
This article has not been copyedited and formatted. The final version may differ from this version.



anthelmintic drugs such as levamisole, pyrantel and morantel (Harrow and Gration, 1985; Jones et al., 2005).

The most detailed available structure of a native nAChR in situ has been determined by electron microscopy of tubular crystals of *Torpedo marmorata* postsynaptic membranes embedded in amorphous ice (Miyazawa et al., 1999; Miyazawa et al., 2003); (Unwin, 2005). Models based on these co-ordinates indicate that the extracellular region, containing the ligand-binding site, consists of twisted β-sheets, with loop regions forming the binding sites. In 2001, T. Sixma and colleagues first crystallized a glial-derived acetylcholine binding protein (AChBP) from the freshwater snail, *Lymnaea stagnalis* (Brejc et al., 2001). This 210 amino acid polypeptide forms a stable homo-pentamer with homology to the N-terminal extracellular region of nAChRs. ACh binding sites are located at each of the 5 subunit interfaces and the 6 binding loops (A-F) that can be recognized in nAChRs are also present. Several AChBP crystal structures have now been published (Brejc et al., 2001; Brejc et al., 2002; Celie et al., 2005a; Celie et al., 2005b; Celie et al., 2004b; Hansen et al., 2005). In view of the important structural homology and sequence similarity (24% identity), between the AChBP and the ligand binding domain of neuronal α7 (,homology modeling can offer a useful tool to investigate ligand binding. The structure of the chicken α7 homopentamer has been constructed based on both the X-ray structure of the *L.stagnalis* AChBP and the electron microscopy derived structure of the transmembrane region of the Torpedo nicotinic receptor (Amiri et al., 2005). Le Novère and colleagues have built a three-dimensional model of the N-terminal domain of a homopentameric chicken α7 nAChR based on AChBP, which was then used to analyze the docking of ACh, epibatidine and nicotine (Le Novère et al., 2002). Plausible modes of binding were then suggested for these ligands. In a separate modeling study (Schapira et al., 2002) the binding

Molecular Pharmacology Fast Forward. Published on March 13, 2008 as DOI: 10.1124/mol.107.041590
This article has not been copyedited and formatted. The final version may differ from this version.



affinities were related to different receptor isotypes. During the course of writing this manuscript the crystal structure of the extracellular domain of nAChR α1 subunit bound to α-bungarotoxin at 1.94 A resolution was solved (Dellisanti et al., 2007). Comparisons between the α1 andAChBP structures suggests that AChBP is indeed a good model for the extracellular ligand-binding domain (Dellisanti et al., 2007).

Photoaffinity labeling studies on the molluscan AChBP showed that Y195 in loop C and M116 of loop E interact with the agonist azidoepibatidine (Tomizawa et al., 2007). Mutagenesis studies have previously shown that the equivalent residue in loop E of vertebrate muscle non-α subunits is involved in ligand binding (Sine, 1997). We have generated homology models of the chicken α7 homopentameric nAChR, $(\alpha7)_5$ and show how *in silico* methods combined with site-directed mutagenesis yield further evidence that the corresponding loop E residue of α7, Leu 117, controls ligand access to the agonist-binding site. We also show that this residue is important in the actions on α7 of the insecticide imidacloprid and its derivative desnitro-imidacloprid.

## Materials and Methods.

### *Modeling*

A pairwise sequence alignment for chicken α7 and AChBP (PDB code 1UX2, which has HEPES buffer bound) was generated on the basis of multiple sequence alignments extracted from the pfam database (Bateman et al., 2002) and improved by manual adjustment. The alignment (Figure 1A) was used as input for the program MODELLER (Sali and Blundell, 1993) to generate 100 initial pentameric models of the chick α7 ligand binding domain. The quality of the 5 lowest energy structures was checked with the PROCHECKv3.5.4 program

Molecular Pharmacology Fast Forward. Published on March 13, 2008 as DOI: 10.1124/mol.107.041590
This article has not been copyedited and formatted. The final version may differ from this version.



(Laskowski et al., 1993) and the WHAT-IF (http://www.cmbi.kun.nl/gv/servers/WIWWWI) server. The model with the lowest percentage of residues in the disallowed region of the Ramachandran plot was selected for docking studies. Only one binding site from 2 adjacent subunits was used (see Figure 1B). *In silico* site-directed mutagenesis was performed using PyMOL (DeLano, 2004). These structures were deployed as potential docking targets for ACh and imidacloprid usingthe program, Autodock (Morris et al., 1998). Autodock was run with default parameters except that atom types were not set for the ligand but rather according to charges calculated as below. The active site was defined as a radius of (default) 15.0 Å from carbon 6 (IUPAC/IUBMB numbering) of the sidechain of Trp148, a residue located centrally in the ACh binding pocket. The charges on ACh were assigned according to a previous report ((Segall et al., 1998). Charges for imidacloprid were calculated with the 6-31G* basis set using Spartan (Wavefunction Inc). All docking results were visualized with VMD (Humphrey et al., 1996) and UCSF Chimera (Pettersen et al., 2004).

Molecular dynamics simulations were carried out with GROMACS v 3.1.4 (Berendsen *et al.*, 1995; Lindahl *et al*, 2001) using the GROMOS96 (van Gunsteren et al., 1996) force-field. Each system was energy-minimized until convergence using a steepest descents algorithm. Molecular dynamics with position restraints for 100 ps was performed followed by equilibration for 1 ns and finally the production run of 10 ns. During the equilibration phase the temperature and pressure were coupled using the Berendsen methods (Berendsen et al., 1984). During the production runs the Paranillo-Rahman (Parinello and Rahman, 1981) method was used for pressure coupling and the temperature was coupled using the Nosé-Hoover (Nose, 1984) method at 310 K. Electrostatics were calculated with the Particle Mesh Ewald (PME) method (Darden et al., 1993). The LINCS algorithm (Hess et al., 1997) was used to constrain bond

Molecular Pharmacology Fast Forward. Published on March 13, 2008 as DOI: 10.1124/mol.107.041590
This article has not been copyedited and formatted. The final version may differ from this version.



lengths and a time step of 2 fs was used throughout. All calculations were performed on a PIII intel machine running linux kernel 2.4.19smp.

*Electrophysiology on recombinant wild type and mutant α7 receptors*

*Xenopus laevis* oocytes were prepared and injected with cDNA (*Gallus gallus* α7 cDNA in pMT3) as previously described (Shimomura et al., 2003). Membrane currents were recorded by the two-electrode voltage-clamp method using 2.0 M KCl-filled electrodes (resistances 0.5 – 5.0 MΩ) and a GENECLAMP 500B amplifier (Molecular Devices, Sunnyvale, CA, U.S.A.). The oocyte membrane was clamped at –100 mV. Oocytes secured in a Perspex recording chamber (80 µl volume) were perfused continuously at 7-10 ml $min^{-1}$ by a gravity-fed system with standard oocyte saline (SOS) composed of the following (in mM); NaCl 100, KCl 2.0, $CaCl_2$ 1.8, $MgCl_2$ 1.0 and HEPES 5.0, pH 7.6. All the test compounds were dissolved in SOS and bath-applied to oocytes at intervals of 3-5 min to minimize the effects of desensitization. Only oocytes which gave stable responses to two or more successive applications of 200 or 400 µM ACh were used. Concentration-response data were obtained by applying increasing concentrations of agonist to the oocytes. The maximum amplitude of the current recorded in response to each application was normalized to the response to 1 mM ACh. As the concentration-response curves for ACh and imidacloprid were changed by the mutations L118D and L118E, data from mutants were normalized using the current response to 3 mM ACh while data from L118K and L118R mutants were normalized using the response to 3 mM imidacloprid. Using Graph Pad 'Prism' (Graphpad Software, UK), normalized data were fitted as previously described (Shimomura et al., 2003).

Molecular Pharmacology Fast Forward. Published on March 13, 2008 as DOI: 10.1124/mol.107.041590
This article has not been copyedited and formatted. The final version may differ from this version.



*Binding assay for oocyte membranes expressing recombinant wild type and mutant α7 receptors*

The reaction mixtures (50 µl) containing membrane fraction (2 µg), [$^3$H]ACh (31.25-750 µM), atropine (0.5 µM) and paraoxon (10 µM) were incubated for 1 h at room temperature before the reaction was stopped by filtering through a glass filter GF/C (Whatman International Ltd, Maidstone, England) pre-wetted with sodium phosphate buffer (10mM, pH 7.4) containing sodium chloride (50mM) and polyethyleneimine (0.1% (v/v). The glass filters were immediately washed with 1.5 ml sodium phosphate buffer (10mM, pH 7.4) containing sodium chloride (50mM), followed by two washes with 5 ml of the same buffer. Each glass filter was then transferred to 3ml Aquasole-2 (Packard Instrument Co,Meriden, CT) in a glass vial to measure radioactivity using a liquid scintillation counter (LSC-5100, Aloka Co, Ltd, Tokyo, Japan). Specific binding was defined as the difference of the [$^3$H]ACh binding to the membrane fractions from oocytes expressing recombinant nAChRs and those from vector-injected oocytes. Ligand binding assays were performed in at least triplicate (n=3-11). The Kd values were calculated from the saturation curves using PRISM software (Graphpad software Inc., CA).

Molecular Pharmacology Fast Forward. Published on March 13, 2008 as DOI: 10.1124/mol.107.041590
This article has not been copyedited and formatted. The final version may differ from this version.



## Results

*Wild-type α7 model.*

We generated three-dimensional models of the wild-type chicken α7 nAChR. We found that L118, which is locatedin loop E (Corringer et al., 2000b), is situated close to the ligand binding site (Figure 1B) and consequently may influence ligand-protein interactions. We performed docking of ACh, imidacloprid (IMI) and desnitro-imidacloprid (DN-IMI) to the wild-type model. We found that the ACh solutions were tightly clustered (only 4 clusters) in the binding pocket (Figure 2A) and spanned an energy range of 0.3 kcals/mol, but for IMI there were several binding modes in a several clusters (Figure 2B), not all of which were in the immediate binding pocket (7 out of 13 clusters were within an energy cut-off of 1.5 kcals/mol of the lowest energy dock). DN-IMI docking also found the binding pocket but several binding modes were again possible with 6 out of 9 clusters within an energy cut-off of 1.5 kcals/mol of the lowest energy dock (Figure 2C). The energies of the IMI and DN-IMI docks were comparable, but all approximately 3 kcals/mol less than the ACh docks. A comparison of the ACh docking with the crystal structure of carbamylcholine with AChBP (Figure 3A) revealed that the mode of binding is very similar and thus gave us confidence that the procedure could be used further to predict the interactions of ACh with receptor mutants. However, as the solutions found for IMI and DN-IMI were numerous and there is currently no structural information to confirm the docking solutions, we did not have confidence that the procedure could make reliable predictions for these compounds. Furthermore, there is evidence that the receptor can undergo substantial movement of residues in the binding pocket (Henchman et al., 2003) and given the size of IMI (and DN-IMI) we reasoned that the pocket may have to undergo substantial movement to accommodate these molecules.

Molecular Pharmacology Fast Forward. Published on March 13, 2008 as DOI: 10.1124/mol.107.041590
This article has not been copyedited and formatted. The final version may differ from this version.



We therefore examined ACh docking to mutant receptors and performed the following *in silico* mutagenesis on this position; L118E, L118D, L118K and L118R. The results for ACh docking are shown in Figure 3 and for both the L118D mutation (Figure 3B) and the L118E mutation (Figure 3C) the mode of docking resembles that seen for the wild-type receptor (Figure 3A). There is a slight shift in the position of ACh towards what would be the surface of the membrane in the nAChR molecule. This presumably stems from the increased negative charge at L118 which pulls the quaternary nitrogen moiety further downwards compared to wild-type. When we tried to dock ACh to the L118K and L118R mutants, we found that ACh would generally not dock into the binding pocket. In the case of L118K, there were 3 clusters that positioned ACh near the binding pocket but in completely the wrong orientation. The effect was even more marked for the L118R mutation where not one ACh docking was even in the binding pocket. These studies suggested that negatively charged mutations at this position would retain ACh binding, but positively charged mutations would impairACh binding.

*Molecular Dynamics and Multiple Docking*

Before embarking on experiments to confirm these predictions we decided to examine how robust the homology models were to local fluctuations. We were also interested in exploring the consequence of mutations on the stability of the structure. 10 ns Molecular Dynamics (MD) simulations for the wildtype and mutant α7 subunits were therefore performed. A common method for analyzing the relative stability of protein simulations is to analyze the root mean square fluctuations (RMSF) of the Cα atoms. Analysis of the RMSF for AChBP molecules revealed that the mutant structures showed a higher mean RMSF (Figure 4A-D), indicating that this residue has a large influence on the dynamics of the protein. In particular the

Molecular Pharmacology Fast Forward. Published on March 13, 2008 as DOI: 10.1124/mol.107.041590
This article has not been copyedited and formatted. The final version may differ from this version.



regions corresponding to loop E (residues 112-119) appear to exhibit larger fluctuations compared to wild-type. In the case of L118D and L118E there are also increased fluctuations for loop C.

As the result of an MD simulation is to produce a series of coordinates versus time, this presents a means to test the model and the sensitivity of the docking of ACh with respect to local fluctuations of the model. In order to do this we took 100 snapshots from the simulation, one every 100 ps. We then docked ACh back into these snapshots to assess how well the binding pocket retained its shape and ability to accommodate ACh. This analysis showed that the results observed for the starting model were maintained throughout the simulation (see typical snapshots taken from frames at 5 ns in Figure 5A-C), suggesting that small, local residue fluctuations were not critical in determining the pattern of binding. Docking of ACh to snapshots from the wild-type, L118D and L118E resulted in solutions that were both in the binding pocket and had an orientation consistent with carbamylcholine bound to AChBP (Celie et al., 2004a; Celie et al., 2004b). Conversely, L118K and L118R mutant models failed to produce docking solutions with ACh in the binding pocket. Thus, results from the *in-silico* study suggested that the negatively - charged mutations (L118D and L118E) would retain the ability to bind ACh, but the positively - charged mutations (L118K and L118R) would not.

*Electrophysiological studies on wild type and Leu118 mutated α7 nAChRss.*

We investigated the effects of L118D, L118E, L118K and L118R substitutions on the functional α7 nAChR expressed in *Xenopus laevis* oocytes. Control experiments on wild-type α7 show that imidacloprid is a partial agonist (Figure 6A) consistent with earlier experiments (Matsuda et al., 2000). Figures 6B and 6C show that following the L118D and L118E

Molecular Pharmacology Fast Forward. Published on March 13, 2008 as DOI: 10.1124/mol.107.041590
This article has not been copyedited and formatted. The final version may differ from this version.



mutations, responses of the α7 receptor to imidacloprid were abolished ($P<0.01$ using a one-way ANOVA Dunnett's multiple comparison test). However, the α7 mutants still responded to ACh (Figure 6B, 6C). The $EC_{50}$ values of ACh were increased by these two mutations (Table 1). In complete contrast to the findings for the L118D and L118E mutations, L118K and L118R mutations blocked the responses to ACh, whereas responses to imidacloprid were observed (Figures 6D and 6E). In addition to these striking effects on the responses to ACh and imidacloprid, the mutations of L118 slowed the desensitization of the responses.

Desnitro-imidacloprid (DN-IMI) is a derivative of imidacloprid lacking the nitro group. The guanidine moiety of this compound is protonated at neutral pH (Figure 1C). The maximum response to DN-IMI of the wild-type α7 nAChR expressed in *Xenopus* oocytes, was slightly greater than the response to ACh (Figure 7A), resembling results of a previous study (Ihara et al., 2003). The L118D and L118E mutations did not significantly affect the maximum response of α7 to DN-IMI (Figures 7B and 7C) (Table 2). However, the concentration-response curve of DN-IMI was shifted to the right by the L118D and L118E mutations (Table 1). In contrast to the effects on the maximum response to imidacloprid, the L118K and L118R mutations abolished the nicotinic receptor response to DN-IMI (Figures 7D and 7E). Thus the $pEC_{50}$ values for DN-IMI could not be determined for these two mutant receptors

The concentration-response curves of ACh, imidacloprid and DN-IMI for the wild-type (A) and L118D (B), L118E (C), L118K (D) and L118E (E) mutants are shown in Figure 8. It could be argued that in certain mutants imidacloprid may antagonise the response to ACh and ACh may antagonise the actions of imidacloprid. To begin to address this, we have examined if the response to imidacloprid of the L118R mutant and, similarly, the response to ACh of the L118D mutant are suppressed by co-application with ACh and imidacloprid, respectively. It

Molecular Pharmacology Fast Forward. Published on March 13, 2008 as DOI: 10.1124/mol.107.041590
This article has not been copyedited and formatted. The final version may differ from this version.



was found that the response to 1 mM imidaclolprid in loop E was suppressed by co-application with 1 mM ACh to 0.306 ± 0.099 (N=2) as compared with the response (=1.00) to 1 mM imidaclolprid alone. On the other hand, the response to 3 mM ACh of the L118D mutant was suppressed by co-application with 1 mM imidacloprid to 0.721 ± 0.125 (N=2) as compared with the response (=1.00) to 3 mM ACh alone.

*Radioligand binding studies on wild type and mutant α7 nAChRs*

Binding experiments were also conducted to evaluate the affinity of [$^3$H]ACh for the oocyte membrane fractions including the recombinant wild type and mutant α7 nAChRs. [$^3$H]ACh showed saturable binding to the membrane fractions (Fig. 9). The Kd values (mean ± sem) of ACh for the wild type, L118R and L118D were 211.4 ± 56.9 μM, 538.6 ± 285.1 μM and 109.5 ± 64.1 μM, respectively. The Kd value of [$^3$H]imidaclolprid could not be determined because of its low binding affinity (data not shown).

**Discussion.**

Our prediction of ACh-nAChR interaction for several mutants at position L118 of α7 is supported by the *in vitro* experiments, suggesting that this model is capable of capturing the effects of ACh interacting with homomeric α7 nAChRs. A previous report also highlights the involvement of the corresponding residue in ligand binding where L119C, L119C and L121C mutants of the vertebrate muscle nAChR subunits γ, ε and δ, respectively, treated with aminoethyl methanethiosulfonate showed reduced affinity for dimethyl-*d*-tubocurarine and α-conotoxin M1 (Sine, 1997). Similar results were observed for the γL119K, εL119K and δL121K mutants. Also, using photoaffinity labeling a methionine (M116) at the equivalent position in loop E of another molluscan AChBP from Aplysia was shown to be involved in

Molecular Pharmacology Fast Forward. Published on March 13, 2008 as DOI: 10.1124/mol.107.041590
This article has not been copyedited and formatted. The final version may differ from this version.



imidacloprid binding (Tomizawa et al., 2007). All these findings indicate that the pyridine ring of imidacloprid is likely to interact with loop E, placing its nitro group so as to interact with other residues facing the agonist binding domain.

Several studies have shown that electrostatic forces are important for imidacloprid interaction with nAChRs (Ihara et al., 2007; Sattelle et al., 2005). Here we show that substitutions of L118 in loop E by acidic or basic residues strikingly influence the responses of α7 to ACh. It should be noted that the antagonist action of ACh on the response of the L118D mutant to 1 mM imidacloprid was not sufficiently potent to block the response completely. A possible simple explanation for the effects of such mutations is that if L118 is mutated to a positive side-chain, the interaction with the charged quaternary nitrogen may be strong enough to prevent binding to the pocket and as a result the channel fails to open. We have confidence that our model of $(\alpha 7)_5$ is reasonable due to the fact that a similar orientation of ACh to that found for carbamylcholine in AChBP (Celie et al., 2004a) was predicted. Furthermore, our model seems robust to small local changes in residue conformation as exemplified by the molecular dynamics (Figure 4). In addition, the recent structure of the α1 nAChR subunit ligand-binding domain (Dellisanti et al., 2007) suggests that AChBP provides a suitable template for modeling the extracellular domain in this way.

Our initial model did not allow us to make confident predictions about the interactions of imidacloprid with the $(\alpha 7)_5$ model. This is perhaps not too surprising given that our model is based upon AChBP with HEPES bound. If the receptor conforms to an induced-fit model in terms of its interactions with ligands, then the model will suffer from being biased away from a conformation that would bind imidacloprid. Furthermore, recent experiments on AChBP (Gao et al., 2005) and on homology models of α7 (Henchman et al., 2003; Henchman et al., 2005)

Molecular Pharmacology Fast Forward. Published on March 13, 2008 as DOI: 10.1124/mol.107.041590
This article has not been copyedited and formatted. The final version may differ from this version.



suggest that there can be substantial changes in the shape of the binding pocket, in particular the conformation of loop C.

However, taking all these factors into consideration along with our present findings, we propose a model that accounts for the data shown in Figures 6 and 7. Imidacloprid has a negatively charged nitro group whilst its desnitro derivative (DN-IMI) possesses a positive charge at the guanidine moiety. It is interesting to note that the effects of mutations on DN-IMI are quite similar to those seen for ACh. Thus it could be that the position of their positive charges in the binding pocket are similar. However, that would presumably require a different conformation of loop C in order to allow the DN-IMI to adopt a sterically favourable position within the binding pocket. Imidacloprid itself fails to generate currents in L118D and L118E mutants, but can effect channel opening in the case of L118K and L118R mutants. However, imidacloprid modulated the ACh-induced response of the L118D mutant, suggesting that the electrostatic interaction between the nitro group and this residue is critical in determining whether it will permit channel opening in response to agonist binding. A similar explanation is possible for the action of ACh on the mutant receptors. The L118 mutations influenced the desensitization of the imidacloprid- and ACh-induced responses, reflecting the role for L118 in the channel gating mechanism.

Electrostatic interactions are not the only forces determining agonist interactions with the α7 nAChR. The L118D and L118E mutations shifted the ACh concentration-response curve to higher concentrations and slightly reduced the maximum current amplitudes observed in response to ACh (Figure 8), suggesting that such mutations in loop E may lead indirectly to a conformational change in another region of the receptor playing a key role in interactions with agonists. Thus, it will be necessary to further improve the modeling to gain a more complete

Molecular Pharmacology Fast Forward. Published on March 13, 2008 as DOI: 10.1124/mol.107.041590
This article has not been copyedited and formatted. The final version may differ from this version.



understanding of neonicotinoid-nAChR interactions. Nevertheless, electrostatic interactions can explain the changes in concentration-response curves of the imidacloprid derivative DM-IMI lacking the nitro group. Unlike imidacloprid, DN-IMI has a positive charge at the guanidine moiety, thereby mimicking ACh. Consistent with this, the L118K and L118R mutations abolished responses of the α7 nAChR to DN-IMI, whereas L118D and L118E mutations permitted the agonist actions of this ligand.

Leu118 is not highly conserved across the nAChR family. Thus, the residue at this location may participate in determining subunit-specific responses to agonists. In the Drosophila Dβ2 subunit, the residue corresponding to Leu118 is glutamic acid (Table 2). Since we found that the L118E mutation in α7 abolished imidacloprid action while retaining sensitivity to ACh, it is predicable that imidacloprid will not be efficacious on insect nAChRs containing Dβ2 subunit in opening the channel gate. Conversely, several other insect nAChR subunits, such as *Drosophila melanogaster* Dα1, Dα3 and Dα4 as well as *Myzus persicae* α2 and α3 possess either an arginine or lysine at the position corresponding to Leu118 (Table 2), which in our site-directed mutagenesis experiments increased the efficacy of imidacloprid (Table 1). Interestingly, studies have indicated that these subunits play a role in determining sensitivity to the insecticide, imidacloprid (Huang et al., 1999; Lansdell and Millar, 2000; Matsuda et al., 2001a; Shimomura et al., 2002; Shimomura et al., 2003; Shimomura et al., 2004; Shimomura et al., 2006). Even though it is thought that in heteromeric nAChRs consisting of α and β subunits, loop E from the β subunit contributes to the agonist binding site (Corringer et al., 2000b), it is important to note that the subunit composition and stoichiometry of native insect nAChRs have yet to be determined. Such information will prove instructive in assessing the relevance of loops A-F of either α or β subunits in agonist binding and hence neonicotinoid sensitivity. Also, mutations at

Molecular Pharmacology Fast Forward. Published on March 13, 2008 as DOI: 10.1124/mol.107.041590
This article has not been copyedited and formatted. The final version may differ from this version.



L118 may provide a route by which target-site resistance could develop. If it is the case that in several insect nAChR α subunits, the arginine or lysine at the residue corresponding to L118 contributes to imidacloprid sensitivity, a simple negative charge mutation here would be enough to maintain responses to the natural agonist, ACh, while abolishing the agonist actions of imidacloprid. Thus in searching field strains resistant to imidacloprid, it may be of interest to look for changes in loop E as well as the important loop B mutations (Liu et al., PNAS) already known to be associated with imidacloprid resistance.

In conclusion, we have used molecular modeling to predict that Leu118 of the α7 nAChR subunit contributes to agonist binding. Site-directed mutagenesis and functional expression of wild-type and mutant nAChRs subsequently confirmed this prediction. These results, taken together with our previous studies on loops C, D and F (Shimomura et al., 2002; Shimomura et al., 2006; Shimomura et al., 2004; Shimomura et al., 2003) are enhancing our understanding of the binding to nAChRs of commercially important nicotinic agonists.

Molecular Pharmacology Fast Forward. Published on March 13, 2008 as DOI: 10.1124/mol.107.041590
This article has not been copyedited and formatted. The final version may differ from this version.



**Acknowledgements.**

We thank M. Ballivet for kindly providing the chicken α7 cDNA.

Molecular Pharmacology Fast Forward. Published on March 13, 2008 as DOI: 10.1124/mol.107.041590
This article has not been copyedited and formatted. The final version may differ from this version.



## References

Amiri S, Tai K, Beckstein O, Biggin PC and Sansom MS (2005) The alpha7 nicotinic acetylcholine receptor: molecular modelling, electrostatics, and energetics. *Mol Membr Biol* **22**(3):151-162.

Bateman A, Birney E, Cerruti L, Durbin R, Etwiller L, Eddy SR, Griffiths-Jones S, Howe KL, Marshall M and Sonnhammer EEL (2002) The pfam protein families database. *Nucleic Acids Res* **30**:276-280.

Berendsen HJC, Postma JPM, van Gunsteren WF, DiNola A and Haak JR (1984) Molecular dynamics with coupling to an external bath. *J Chem Phys* **81**:3684-3690.

Brejc K, van Dijk WJ, Klassen RV, Schuurmans M, van Der Oost J, Smit AB and Sixma TK (2001) Crystal structure of an ACh-binding protein reveals the ligand-binding domain of nicotinic receptors. *Nature* **411**:269-276.

Brejc K, van Dijk WJ, Smit AB and Sixma TK (2002) The 2.7 Å structure of AChBP, homologue of the ligand-binding domain of the nicotinic acetylcholine receptor. *Novartis Found Symp* **245**:22-29.

Celie PH, Kasheveroc IE, Mordvintsev DY, Hogg RC, van Nierop P, van Elk R, van Rossum-Fikkert SH, Zhmak MN, Bertrand D, Tsetlin V, Sixma TK and Smit AB (2005a) Crystal strucutre of nicotinic acetylcholine receptor homolog AChBP in complex with an alpha-conotoxin PnIA variant. *Nat Struct Mol Biol* **12**:582-588.

Celie PH, Klassen RV, van Rossum-Fikkert SH, van Elk R, van Nierop P, Smit AB and Sixma TK (2005b) Crystal structure of acetylcholine-binding protein from Bulinus truncatus reveals the conserved structural scaffold and sites of variation in nicotinic acetylcholine receptors. *J Biol Chem* **280**:26457-26466.

Celie PH, van Rossum-Fikkert SE, van Dijk WJ, Brejc K, Smit AB and Sixma TK (2004a) Nicotine and carbamylcholine binding to nicotinic acetylcholine receptors as studied in AChBP crystal structures. *Neuron* **41**(6):907-914.

Celie PH, van Rossum-Fikkert SH, van Dijk WJ, Brejc K, Smit AB and Sixma TK (2004b) Nicotine and carbamylcholine binding to nicotinic acetylcholine receptors as studied in AChBP crystal structures. *Neuron* **41**:907-914.

Changeux J-P and Edelstein SJ (2001) Allosteric mechanisms in normal and pathological nicotinic acetylcholine receptors. *Curr Opin Neurobiol* **11**:369-377.

Corringer P-J, Le Novere N and Changeux J-P (2000a) Nicotinic receptors at the amino acid level. *Annu Rev Pharmacol Toxicol* **40**:431-458.

Corringer P-J, Le Novère N and Changeux J-P (2000b) Nicotinic receptors at the amino acid level. *Annu Rev Pharmacol Toxicol* **40**:431-458.

Darden T, York D and Pedersen L (1993) Particle mesh Ewald - an N.log(N) method for Ewald sums in large systems. *J Chem Phys* **98**(12):10089-10092.

DeLano WL (2004) The PyMOL molecular graphics system. *DeLano Scientific LLC, San Carlos, CA UDA.*

Dellisanti CD, Yao Y, Stroud JC, Wang ZZ and Chen L (2007) Crystal structure of the extracellular domain of nAChR alpha1 bound to alpha-bungarotoxin at 1.94 A resolution. *Nat Neurosci* **10**(8):953-962.

Gao F, Bren N, Burghardt TP, Hansen SB, Henchman RH, Taylor P, McCammon JA and Sine SM (2005) Agonist-mediated conformational changes in acetylcholine-binding potein revealed by simulation and intrinsic tryptophan fluorescence. *J Biol Chem* **280**:8443-8451.

Hansen SB, Sulzenbacher G, Huxford T, Marchot P, Taylor P and Bourne Y (2005) Structures of the Aplysia AChBP complexes with nicotinic agonists and antagonists reveal distinctive binding interfaces and conformations. *EMBO J*:1-12.

Harrow ID and Gration KAF (1985) Mode of action of the anthelmintics morantel, pyrantel and levimisole on muscle cell membrane of the nematode Ascatis suum. *Pesti Sci* **16**:662-672.

Henchman RH, Wang H-L, Sine SM, Taylor P and McCammon JA (2003) Asymmetric structural motions of the homomeric a7 nicotinic receptor ligand binding domain revealed by molecular dynamics simulation. *Biophys J* **85**:3007-3018.

Henchman RH, Wang HL, Sine SM, Taylor P and McCammon JA (2005) Ligand-induced conformational change in the alpha7 nicotinic receptor ligand binding domain. *Biophys J* **88**(4):2564-2576.

Hess B, Bekker J, Berendsen HJC and Fraaije JGEM (1997) LINCS: A linear constraint solver for molecular simulations. *J Comp Chem* **18**:1463-1472.

Huang Y, Williamson MS, Devonshire AL, Windass JD, Lansdell SJ and Millar NS (1999) Molecular characterization and imidacloprid selectivity of nicotinic acetylcholine receptor subunits from the peach-potato aphid *Myzus persicae*. *J Neurochem* **73**(1):380-389.

Humphrey W, Dalke A and Schulten K (1996) VMD - Visual molecular dynamics. *J Molec Graph* **14**:33-38.

Ihara M, Shimomura M, Ishida C, Nishiwaki H, Akamatsu M, Sattelle DB and Matsuda K (2007) A hypothesis to account for the selective and diverse actions of neonicotinoid insecticides at their molecular targets, nicotinic acetylcholine receptors: catch and release in hydrogen bond networks. *Invert Neurosci* **7**(1):47-51.

Jones AK, Buckingham SD and Sattelle BM (2005) Chemistry-to-gene screens in Caenorhabditis elegans. *Nat Rev Drug Disc* **4**:321-330.

Karlin A (2002) Emerging structure of the nicotinic acetylcholine receptors. *Nat Rev Neurosci* **102**:102-114.

Lang B and Vincent A (2003a) Autoantibodies to ion channels at the neuromuscular junction. *Autoimmun Rev* **2**(2):94-100.

Lang B and Vincent A (2003b) Autoantibodies to ion channels at the neuromuscular junction. *Autoimmun Rev* **2**:94-100.

Lansdell SJ and Millar NS (2000) The influence of nicotinic receptor subunit composition upon agonist, alpha-bungarotoxin and insecticide (imidacloprid) binding affinity. *Neuropharmacology* **39**(4):671-679.

Laskowski RA, Macarthur MW, Moss DS and Thornton JM (1993) PROCHECK - A program to check the stereochemical quality of protein structures. *J Appl Crystall* **26**:283-291.

Le Novère N, Grutter T and Changeux J-P (2002) Models of the extracellular domain of the nicotinic receptors and of agonist- and Ca2+ -binding sites. *Proc Natl Acad Sci* **99**:3210-3215.

Lena C and Changeux J-P (1998) Allosteric nicotinic receptors, human pathologies. *J Physiol Paris* **92**:63-74.

Lloyd GK and Williams M (2000) Neuronal nicotinic acetylcholine receptors as novel drug targets. *J Pharmacol Exp Therapeu* **292**:461-467.

Matsuda K, Buckingham SD, Kleier D, Rauh JJ, Grauso M and Sattelle DB (2001a) Neonicotinoids: insecticides acting on insect nicotinic acetylcholine receptors. *Trends Pharmacol Sci* **22**(11):573-580.

Matsuda K, Ihara M, Nishimura K, Sattelle DB and Komai K (2001b) Insecticidal and neural activities of candidate photoaffinity probes for neonicotinoid binding sites. *Biosci Biotechnol Biochem* **65**:1534-1541.

Matsuda K, Shimomura M, Kondo Y, Ihara M, Hashigami K, Yoshida M, Raymond V, Mongan NP, Freeman JC, Komai K and Sattelle DB (2000) Role of loop D of the alpha7 nicotinic acetylcholine receptor in its interaction with the insecticide imidacloprid and related neonicotinoids. *Br J Pharmacol* **130**:981-986.

Millar NS (2003a) Assembly and subunit diversity of nicotinic acetylcholine receptors. *Biochem Soc Trans* **31**(Pt 4):869-874.

Millar NS (2003b) Assembly and subunit diversity of nicotinic acetylcholine receptors. *Biochem Soc Trans* **31**:869-874.

Miyazawa A, Fujiyoshi Y, Stowell M and Unwin N (1999) Nicotinic acetylcholine receptor at 4.6 Å resolution: Transverse tunnels in the channel wall. *J Mol Biol* **288**(5):765-786.

Miyazawa A, Fujiyoshi Y and Unwin N (2003) Structure and gating mechanism of the acetylcholein receptor pore. *Nature* **424**:949-955.

Morris GM, Goodsell DS, Halliday RS, Huey R, Hart WE, Belew RK and Olson AJ (1998) Automated docking using a Lamarckian genetic algorithm and an empirical binding free energy function. *Journal of Computational Chemistry* **19**(14):1639-1662.

Nose S (1984) A molecular dynamics method for simulations in the canonical ensemble. *Mol Phys* **52**:255-268.

Ohno K and Engel AG (2002) Congenital myasthenic syndromes: genetic defects of the neuromuscular junction. *Curr Neurol Neurosci Rep* **2**(78-88).

Papke RL, Meyer E, Nutter T and Uteshev VV (2000) α7 receptor-selective agonists and modes of α7 receptor activation. *Eur J Pharmacol* **393**:179-195.

Parinello M and Rahman A (1981) Polymorphic transitions in single crystals - a new molecular dynamics method. *J Appl Phys* **52**:7182-7190.

Pettersen EF, Goddard TD, Huang CC, Couch GS, Greenblatt DM, Meng EC and Ferrin TE (2004) USCF chimera - A visualization system for exploratory research and analysis. *J Comp Chem* **25**(13):1605-1612.

Prendergast MA, Jackson WJ, Terry AVJ, Decker MW, Arneric SP and Buccafusco JJ (1998) Central nicotinic receptor agonists ABT-418, ABT-089, and (-)-nicotine reduce distractibility in adult monkeys. *Psychopharmacology (Berl)* **136**:50-58.

Sali A and Blundell TL (1993) Comparative protein modelling by satisfaction of spatial restraints. *J Mol Biol* **234**:779-815.

Sattelle DB, Jones AK, Sattelle BM, Matsuda K, Reenan R and Biggin PC (2005) Edit, cut and paste in the nicotinic acetylcholine receptor gene family of *Drosophila melanogaster*. *Bioessays* **27**(4):366-376.

Schapira M, Abagyan R and Totrov M (2002) Structural model of nicotinic acetylcholine receptor isotypes bound to acetylcholine and nicotine. *BMC Struct Biol* **2**:1-8.

Segall MD, Payne MC and Boyes RN (1998) An ab initio study of the conformational energy map of acetylcholine. *Molec Phys* **93**(3):365-370.

Shimomura M, Okuda H, Matsuda K, Komai K, Akamatsu M and Sattelle DB (2002) Effects of mutations of a glutamine residue in loop D of the alpha7 nicotinic acetlycholine receptor on agonist profiles for neonicotinoid insecticides and related ligands. *Br J Pharmacol* **137**:162-169.

Shimomura M, Yokota M, Ihara M, Akamatsu M, Sattelle DB and Matsuda K (2006) Role in the selectivity of neonicotinoids of insect-specific basic residues in loop D of the nicotinic acetylcholine receptor agonist binding site. *Mol Pharmacol* **70**:1255-63.

Shimomura M, Yokota M, Matsuda K, Sattelle DB and Komai K (2004) Roles of loop C and the loop B-C interval of the nicotinic receptor a subunit in its selective interactions with imidacloprid in insects. *Neurosci Lett* **363**:195-198.

Shimomura M, Yokota M, Okumura M, Matsuda K, Akamatsu M, Sattelle DB and Komai K (2003) Combinatorial mutations in loops D and F strongly influence responses of the α7 nicotinic acetylcholine receptor to imidacloprid. *Brain Research* **991**:71-77.

Sine SM (1997) Identification of equivalent residues in the gamma, delta, and epsilon subunits of the nicotinic receptor that contribute to alpha-bungarotoxin binding. *J Biol Chem* **272**(38):23521-23527.

Steinlein OK (2001) Genes and mutations in idiopathic epilepsy. *Am J Med Genet* **106**:139-145.

Tomizawa M, Maltby D, Medzihradszky KF, Zhang N, Durkin KA, Presley J, Talley TT, Taylor P, Burlingame AL and Casida JE (2007) Defining nicotinic agonist binding surfaces through photoaffinity labeling. *Biochemistry* **46**(30):8798-8806.

Unwin N (2005) Refined Structure of the Nicotinic Acetylcholine Receptor at 4Å Resolution. *J Mol Biol* **346**:967-989.

van Gunsteren WF, Krüger P, Billeter SR, Mark AE, Eising AA, Scott WRP, Hüneberger PH and Tironi IG (1996) Biomolecular simulation: The GROMOS96 manual and user guide, Biomos/Hochschulverlag AG an der ETH Zürich, Groningen/Zürich.

Vernino S and Lennon VA (2003a) Neuronal ganglionic acetylcholine receptor autoimmunity. *Ann N Y Acad Sci* **998**:211-214.

Vernino S and Lennon VA (2003b) Neuronal ganglionic acetylcholine receptor autoimmunity. *Ann NY Acad Sci* **998**:211-214.

Watson R, Jepson JE, Bermudez I, Alexander S, Hart Y, McKnight K, Roubertie A, Fecto F, Valmier J, Sattelle DB, Beeson D, Vincent A and Lang B (2005) Alpha7-acetylcholine receptor antibodies in two patients with Rasmussen encephalitis. *Neurology* **65**(11):1802-1804.

Molecular Pharmacology Fast Forward. Published on March 13, 2008 as DOI: 10.1124/mol.107.041590
This article has not been copyedited and formatted. The final version may differ from this version.



**Footnotes.**

The support of The Medical Research Council of the UK (AKJ, DBS) and The Wellcome Trust (AS, MSPS, PCB) is gratefully acknowledged. RV thanks the Overseas Research Scheme for support. PCB is an RCUK Fellow. KM was supported by the"Academic Frontier" Project for Private Universities from the Ministry of Education, Culture, Sports, Science and Technology of Japan as well as the Integrated Research Project for Plant, Insect and Animal using Genome Technology from the Ministry of Agriculture, Forestry and Fisheries of Japan. KM also acknowledges the support of the program for Basic Research Activities for Innovative Biosciences (Bio-oriented Technology Research Advancement Institution: BRAIN).

Molecular Pharmacology Fast Forward. Published on March 13, 2008 as DOI: 10.1124/mol.107.041590
This article has not been copyedited and formatted. The final version may differ from this version.



**Figure Legends**

**Figure 1.** A) The alignment used with Modeller in order to generate the initial homology model. The positions of the six loops (Loop A-F) involved in ligand binding are indicated. B) Only two of the five subunits were used in the docking and simulations runs. The various loops that have been shown to contribute to binding are highlighted: Loop A (blue), Loop B (yellow), Loop C (pink), Loop D (orange), Loop E (green) and Loop F (red). The position L118 and other key residues involved in ACh-binding are highlight in licorice. C) Chemical structures of the ligands used in this study.

**Figure 2.** Lowest energy docking solutions against the wild-type α7 model for A) ACh (from a total of 4 clusters), B) for IMI (from 7 clusters with 1.5 kcal/mol of the lowest energy solution) and C) for DN-IMI (from 6 clusters within 1.5 kcal/mol of lowest energy solution).

**Figure 3.** A) Dock of ACh to wild-type α7 model (purple) over-layed onto the AChBP-carbamylcholine structure (1UV6, grey). The position of L118 is shown in spacefill representation. B) Docking of ACh to L118D. The principal subunit is shown in grey and the complimentary subunit is in purple. The D118 residue is shown in spacefill and ACh is shown in liquorice. C) Docking of ACh to L118E. The E118 residue is shown in spacefill. There were no docks in the binding pocket for the L118K and L118R mutations.

**Figure 4.** A) RMSFs of wildtype (grey line) compared to the L118D mutation (black line). B) RMSF of wildtype (grey line) compared to L118E (blackline). C) RMSF of wildtype (grey line)

compared to L118K (blackline). D) RMSF of wildtype (grey line) compared to L118R (blackline). The mean of all five subunits in each case is plotted.

**Figure 5.** Docking against snapshots taken from the MD trajectory at 5 ns. Principal subunits are shown in grey and complimentary subunits are shown in purple. A) An example of a dock to snapshot at time = 5 ns for the wild-type. B) An example of a dock to a snapshot at time = 5 ns for the L118D mutation. C) An example of a dock to a snapshot at time = 5 ns for the L118E mutation. The orientation of the docks to these mutants is similar to the solutions found at 0 ns.

**Figure 6.** Maximum current responses of α7 nAChRs to ACh and imidacloprid (IMI). Imidacloprid was a partial agonist, but such an action was completely reduced by L118D (B) and L118E (C) mutations whilst the ACh-induced response was retained. By contrast, L118K (D) and L118R (E) mutations abolished the response to ACh but not to imidacloprid.

**Figure 7.** Maximum current responses of α7 nAChRs to ACh and the desnitro-derivative of imidacloprid, DN-IMI. DN-IMI induced similar current amplitude of the maximum response to ACh of the wild-type nicotinic receptor (A). L118D (B) and L118E (C) mutations retained the DN-IMI-induced response, whereas L118K (D) and L118R (E) mutations markedly reduced it.

**Figure 8.** Concentration-response curves of ACh, imidacloprid and the desnitro-derivative of imidacloprid obtained for wild-type (A), as well as L118D (B), L118E (C), L118K (D) and L118R (E) mutants of the α7 nAChR expressed in *Xenopus laevis* oocytes. Each plot represents

Molecular Pharmacology Fast Forward. Published on March 13, 2008 as DOI: 10.1124/mol.107.041590
This article has not been copyedited and formatted. The final version may differ from this version.



mean ± standard error of the mean of 4-7 experiments using at least two different batches of eggs.

**Fig. 9.** Saturation curve of [$^3$H]acetylcholine to *Xenopus* oocyte membranes expressing the wild-type, L118R and L118D mutant α7 nicotinic acetylcholine receptors. Each point plotted represents the mean with the standard error of the mean shown (n=3-11).

.

**Table 1.** $pEC_{50}$, Imax and Hill coefficient values for acetylcholine, imidacloprid and desnitro-imidacloprid on wild-type and mutant α7 receptors expressed in *Xenopus* oocytes

| | Acetylcholine (ACh) | | | | Imidacloprid | | | | Desnitro-Imidacloprid (DN-IMI) | | | |
|---|---|---|---|---|---|---|---|---|---|---|---|---|
| | Imax[a] | $pEC_{50}$ | Hill | N | Imax | $pEC_{50}$ | Hill | N | Imax | $pEC_{50}$ | Hill | N |
| Wild type | 1.03 ± 0.04 | 3.91 ± 0.05 | 1.4 ± 0.2 | 5 | 0.49 ± 0.03 | 3.63 ± 0.07 | 1.6 ± 0.4 | 6 | 1.21 ± 0.05 | 5.14 ± 0.07 | 1.2 ± 0.2 | 4 |
| L118D | 1.07 ± 0.04 | 2.78 ± 0.04**,[c] | 1.3 ± 0.2 | 4 | ND[b] | ND | ND | 4 | 1.24 ± 0.11 | 4.21 ± 0.11** | 1.5 ± 0.5 | 4 |
| L118E | 0.97 ± 0.02 | 3.12 ± 0.03** | 1.7 ± 0.2 | 7 | ND | ND | ND | 5 | 1.37 ± 0.06 | 4.28 ± 0.08** | 1.6 ± 0.3 | 5 |
| L118K | ND | ND | ND | 4 | 1.14 ± 0.10 | 2.94 ± 0.05** | 2.1 ± 0.4 | 4 | ND | ND | ND | 4 |
| L118R | ND | ND | ND | 5 | 1.07 ± 0.05 | 3.00 ± 0.02** | 2.4 ± 0.4 | 5 | ND | ND | ND | 4 |

a Normalized maximum response. See Methods for details

b Not determined because the response to agonists was not detected or very small.

c Values shown are the result of a fit of the concentration-response data (mean ± standard error of the mean) illustrated in Fig. 8. Statistical test (one-way ANOVA, Dunnett's multiple comparison test) is for significant differences from the wild-type data (** <0.01). The desensitization of the responses were also affected by the mutation.

Molecular Pharmacology Fast Forward. Published on March 13, 2008 as DOI: 10.1124/mol.107.041590
This article has not been copyedited and formatted. The final version may differ from this version.



**Table 2.** Amino acid sequences in loop E. The residue corresponding to L118 of chicken α7 is highlighted in grey shading and basic residues at this position are shown in bold.

| nAChR subunit | Loop E sequence |
|---|---|
| Lymnaea AChBP | GEVLYMPSIRQ |
| Chicken α7 | GHCQYLPPGIF |
| Chicken α4 | GRIKWMPPAIY |
| Chicken β2 | GSIFWLPPAIY |
| Rat β2 | GSIFWLPPAIY |
| Rat β4 | GSIQWLPPAIY |
| Drosophila α1 (ALS) | GKVVW**K**PPAIY |
| Drosophila α2 (SAD) | GKVVWTPPAIF |
| Drosophila α3 | GRVEW**R**PPAIY |
| Drosophila α4 | GLVEW**K**PPAIY |
| Drosophila α5 | GSCLYVPPGIF |
| Drosophila α6 | GSCLYVPPGIF |
| Drosophila α7 | GSCLYVPPGIF |
| Drosophila β1 (ARD) | GEVLWVPPAIY |
| Drosophila β2 (SBD) | GEVFWEPPAIY |
| Drosophila β3 | GHFRWMPPAVY |
| Myzus α1 | GKVMWTPPAIY |
| Myzus α2 | GKVVW**K**PPAIY |
| Myzus α3 | GRVEW**K**PPAIY |
| Myzus α4 | GEVLWSPPAIY |

Figure 1

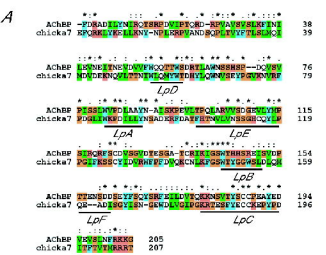
A
AChBP
chicka7
LpD
LpA
LpE
LpB
LpF
LpC
B
W148
L119
Y86
W54
C
acetylcholine
imidacloprid
DN-imidacloprid

Figure 2

A

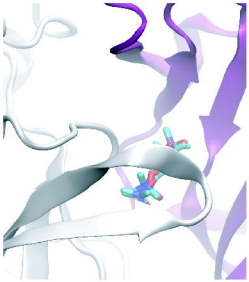

B

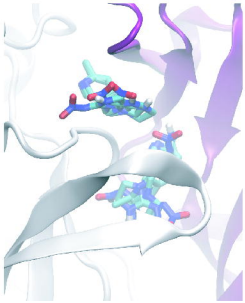

C

Figure 3

A

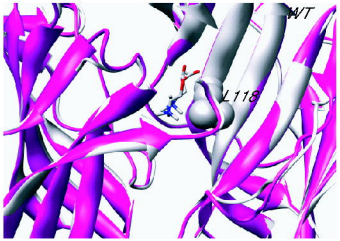


B

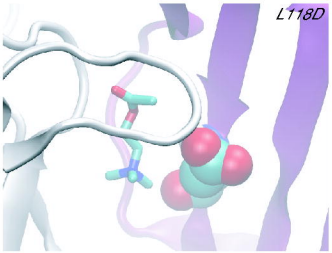


C

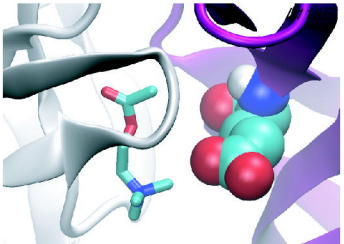

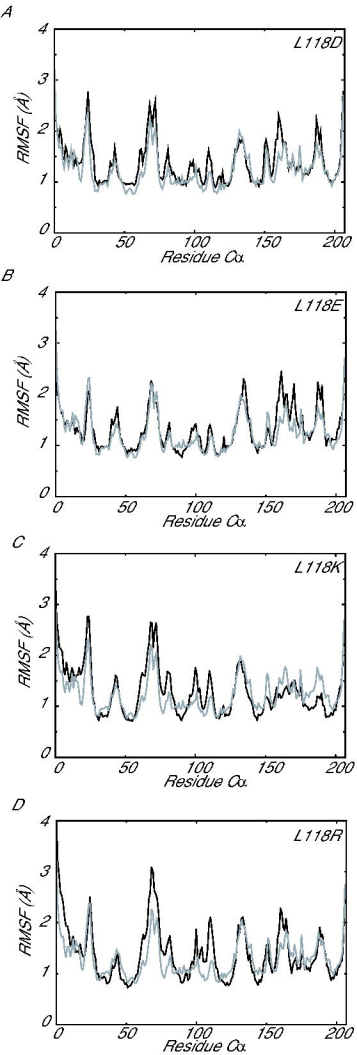
A
L118D
RMSF (Å)
Residue Cα
B
L118E
RMSF (Å)
Residue Cα
C
L118K
RMSF (Å)
Residue Cα
D
L118R
RMSF (Å)
Residue Cα

Figure 5

A

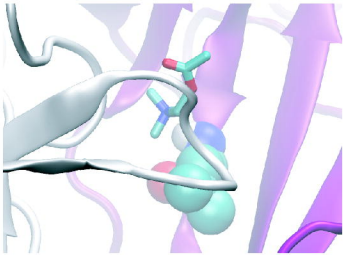

B

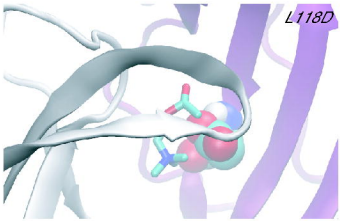


C

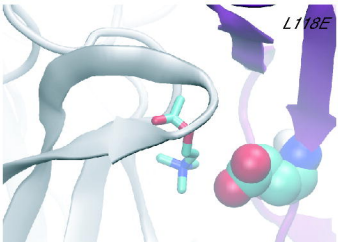

Fig. 6

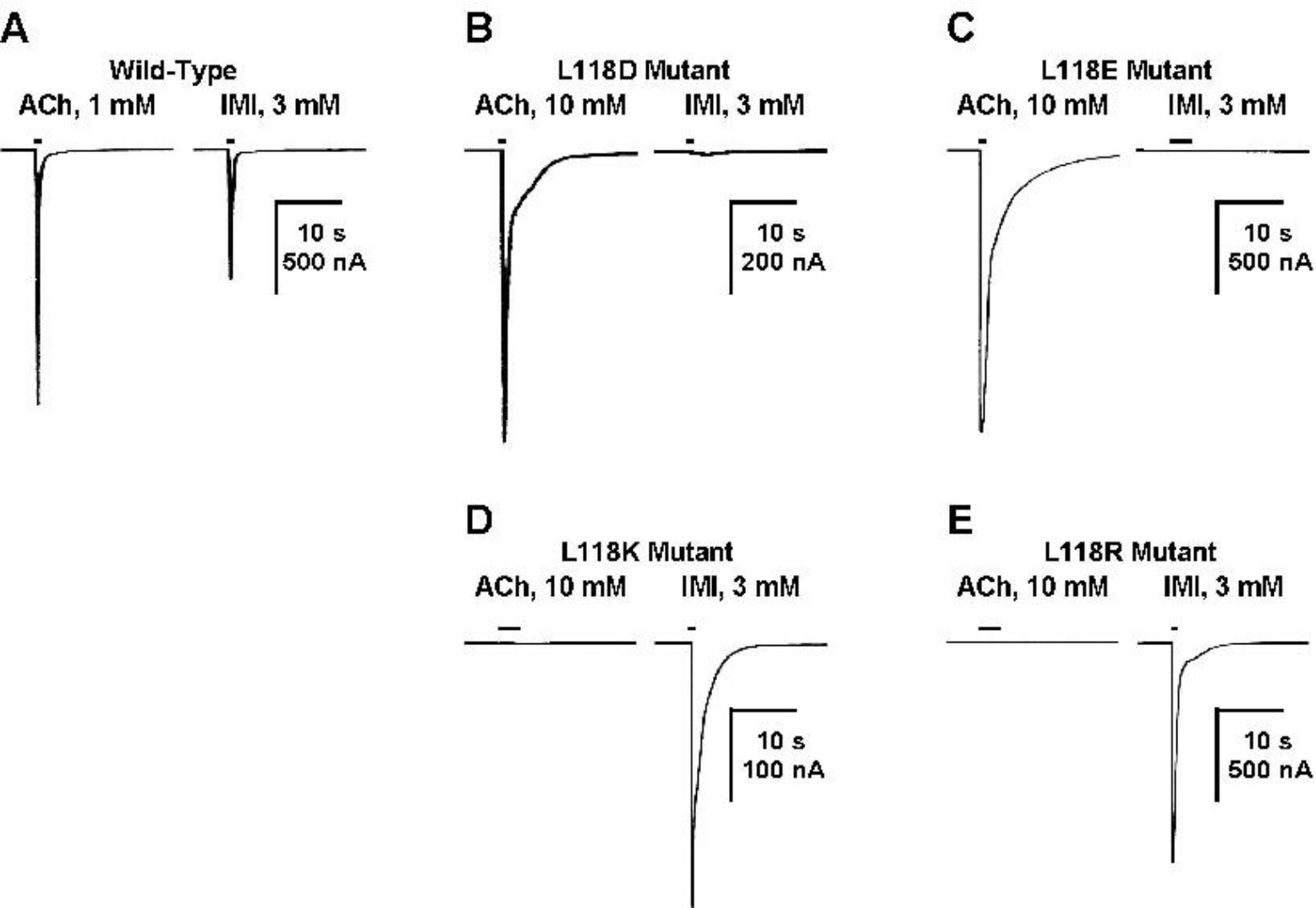
A
Wild-Type
ACh, 1 mM
IMI, 3 mM
10 s
500 nA
B
L118D Mutant
ACh, 10 mM
IMI, 3 mM
10 s
200 nA
C
L118E Mutant
ACh, 10 mM
IMI, 3 mM
10 s
500 nA
D
L118K Mutant
ACh, 10 mM
IMI, 3 mM
10 s
100 nA
E
L118R Mutant
ACh, 10 mM
IMI, 3 mM
10 s
500 nA

Fig. 7

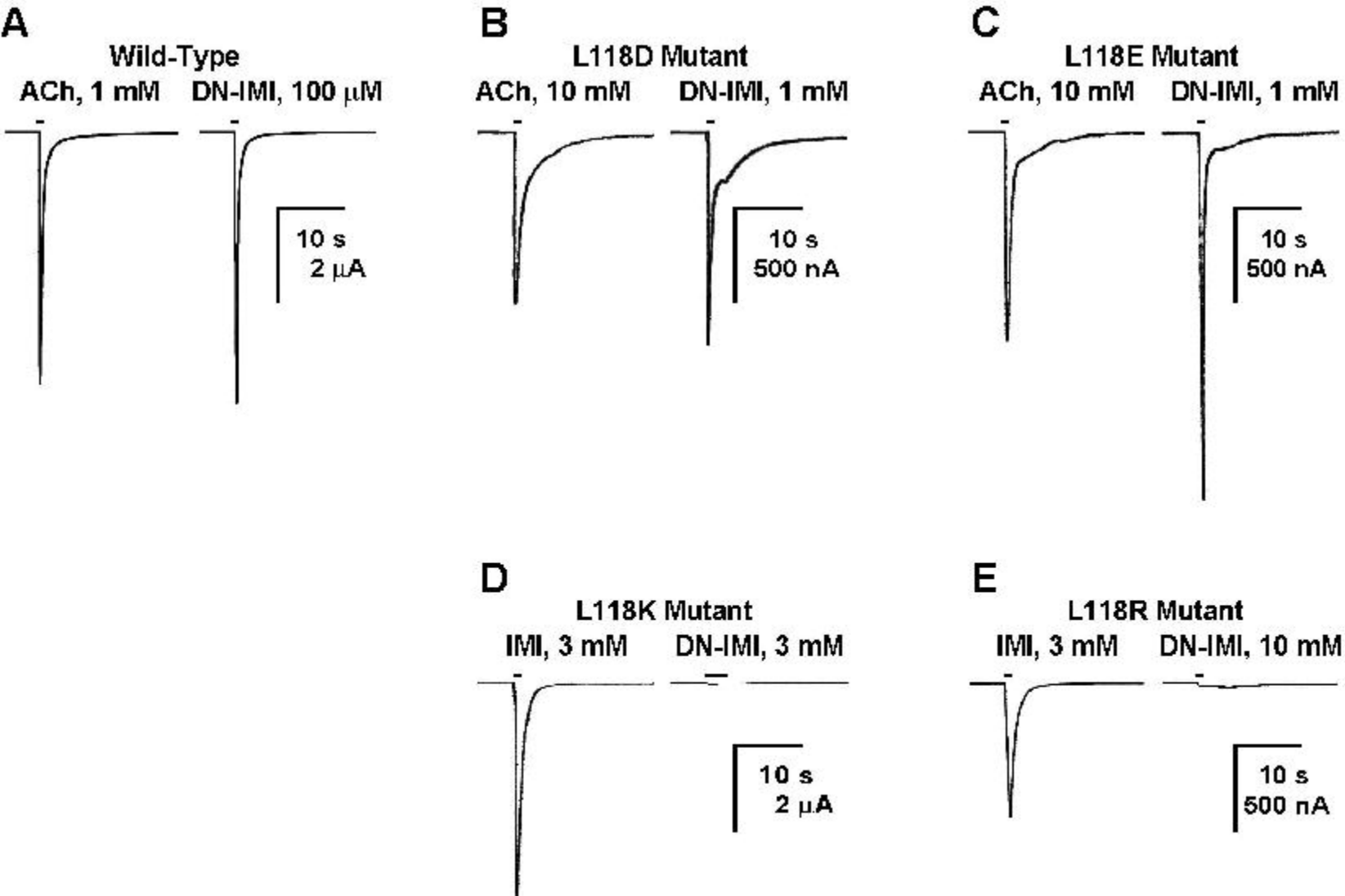
A
Wild-Type
ACh, 1 mM
DN-IMI, 100 μM
10 s
2 μA
B
L118D Mutant
ACh, 10 mM
DN-IMI, 1 mM
10 s
500 nA
C
L118E Mutant
ACh, 10 mM
DN-IMI, 1 mM
10 s
500 nA
D
L118K Mutant
IMI, 3 mM
DN-IMI, 3 mM
10 s
2 μA
E
L118R Mutant
IMI, 3 mM
DN-IMI, 10 mM
10 s
500 nA

Fig. 8

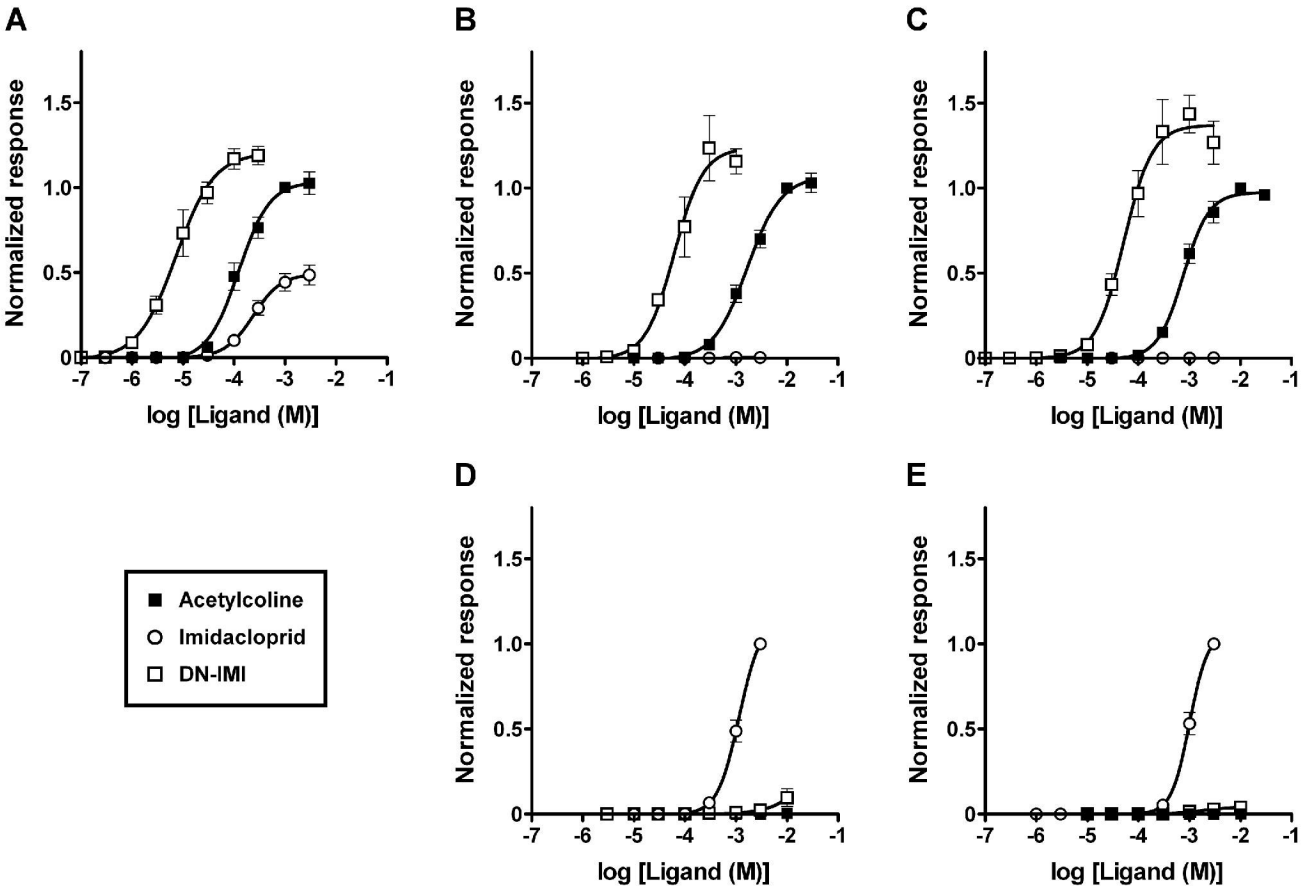
A
B
C
D
E
Normalized response
log [Ligand (M)]
Acetylcoline
Imidacloprid
DN-IMI

Fig. 9

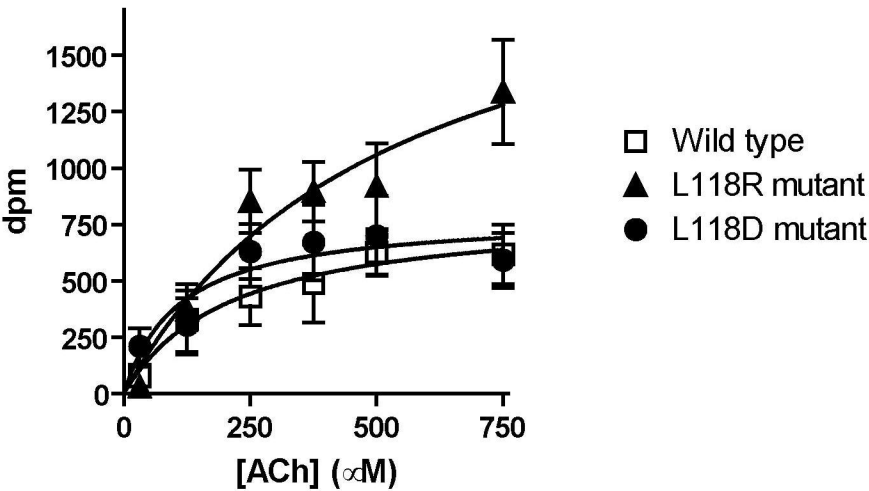
1500
1250
1000
750
500
250
0
dpm
0
250
500
750
[ACh] (∝M)
Wild type
L118R mutant
L118D mutant